frontiers | Frontiers in Materials

TYPE Original Research
PUBLISHED 28 January 2025
DOI 10.3389/fmats.2024.1455648

OPEN ACCESS

EDITED BY
Matteo Becatti,
University of Firenze, Italy

REVIEWED BY
Li Zhang,
Nanjing University, China
Daria Sicari,
PharmaLine srl Italy, Italy

*CORRESPONDENCE
Jinqian Zhang,
jingwanghou@163.com
Chun Feng,
dt0874@163.com

‡These authors have contributed equally to this work

RECEIVED 27 June 2024
ACCEPTED 18 December 2024
PUBLISHED 28 January 2025

CITATION
Cao X, Gong S, Chen S, Hu S, Li T, Guan Y, Feng C and Zhang J (2025) The mechanism of endoplasmic reticulum (ER) stress in cell apoptosis and ROS (reactive oxygen species) of CNE2 cell line induced by single wall carbon nanohorn (SWCNH).
Front. Mater. 11:1455648.
doi: 10.3389/fmats.2024.1455648

The mechanism of endoplasmic reticulum (ER) stress in cell apoptosis and ROS (reactive oxygen species) of CNE2 cell line induced by single wall carbon nanohorn (SWCNH)

Xianbao Cao[1‡], Shunmin Gong[1‡], Shujin Chen[2], Shuang Hu[1], Tianshu Li[1], Yanfei Guan[1], Chun Feng[1*] and Jinqian Zhang [1*]

[1]Department of Otolaryngology Head and Neck Surgery, Yunan Provincial Key Laboratory of Clinical Virology, The First People's Hospital of Yunnan Province, The Affiliated Hospital of Kunming University of Science and Technology, Kunming, Yunnan, China, [2]Department of Otolaryngology Surgery, The Rongchang District People's Hospital, Chongqing, China

Introduction: The interaction between the materials themselves and cancer cells are rarely explored. Therefore, the biological roles of raw single wall carbon nanohorn (SWCNH) on endoplasmic reticulum (ER) stress in the apoptosis of CNE2 were explored.

Methods: Therefore, ERS of CNE2 cells was induced by SWCNH, and 4-phenylbutyrate (4-PBA) was selected as a inhibitor of ERS. CNE2 cells were co-cultured with SWCNH, 4-PBA and SWCNH+4-PBA, respectively. Furthermore, the apoptotic status of CNE2 cells and its ROS (Reactive oxygen species) levels were determined. Moreover, the apoptotic protein expression of caspase 3 (cysteinyl aspartate specific proteinase 3), the expression levels of ER pathway protein eIF2α, ATF4 and CHOP, or the OS (Oxidative stress)-related proteins NQO1, GCLC, HO-1, and Nrf2 was detected, respectively.

Results: CNE2 apoptotic rate, ROS levels, the caspase 3 or ER pathway proteins ATF4 and CHOP expression, even the NQO1, GCLC, HO-1, and Nrf2 levels of oxidative stress-related proteins in the groups of SWCNH and SWCNH+4-PBA were higher compared to the control group. Moreover, these indicators were higher compared to the group of SWCNH+4-PBA ($p < 0.05$).

Discussion: ER stress is the key possible mechanism of CNE2 apoptosis induced by SWCNH. After injury of ERS, SWCNH causes oxidative stress injury, which may eventually lead to apoptosis of CNE2 cells.

KEYWORDS

endoplasmic reticulum stress (ERS), apoptosis, nasopharyngeal carcinoma (NPC), oxidative stress, single-walled carbon nanohorn (SWCNH)

Introduction

The scientists have started the theories and applications of SWCNH (Single-Walled Carbon Nanohorn) (Iijima et al., 1999). Due to its large surface area and specific surface structure, especially its affinity for biomolecules, SWCNH seems to provide biomedical and pharmaceutical prospects. With its closed-tip single-walled nano-scale cavity structure, as well as the advantages of easy dispersion in solvents, uniform size, and high purity, SWCNH maybe the excellent carrier utilizing the drug delivery systems (Murakami and Tsuchida, 2008; Xu et al., 2008; Ajima et al., 2005; Matsumura et al., 2007; Muracami et al., 2008; Ajima et al., 2008).

As an important subcellular structure and functional unit of human body, endoplasmic reticulum (ER) is a common place for many kinds of intracellular and extracellular signal transduction. Under pathological conditions, endoplasmic reticulum stress (ERS) occurs in ER, which produces a large number of unfolded or misfolded proteins and Ca^{2+} balance disorders. Persistent ERS can cause cell dysfunction and trigger oxidative emergency damage (Malhotra and Kaufman, 2007; Lenna et al., 2014). Onoda et al. has confirmed that ERS could be induced by carbon nanoparticles (Onoda et al., 2020). Nasopharyngeal carcinoma (NPC) is an aggressive malignant tumor, especially for patients with recurrent or metastatic NPC. Although platinum-containing induction chemotherapy and radiotherapy is used as the first-line standard treatment, the median progression-free survival of NPC patients is only about 7 months (Iijima et al., 1999). The incidence and mortality of NPC in China are higher than the global average, and the death cases account for about 40% of all patients deaths from NPC in the world (Murakami and Tsuchida, 2008; Chen et al., 2019; Siegel et al. 2021). The etiology of NPC is complex, including genetic susceptibility, Epstein-Barrvirus (EBV) infection, and other environmental risk factors such as smoking, ingestion of preserved foods (Salted fish, etc.), and occupational exposure (Niedobitek, 2000). Recurrence and metastasis are the main reasons for the failure of NPC treatment. GP (Gemcitabine combined with cisplatin) chemotherapy is currently the first-line standard treatment for NPC patients with recurrent or metastatic, but its efficacy is limited and needs to be improved urgently (Zheng et al., 2019).

To provide new treatment strategies for patients with NPC is the crucial significance for accomplishing the improved prognosis of advanced NPC. Therefore, we investigated the bio-effect and mechanism of ERS in apoptosis of CNE2 cell line induced by SWCNH in this work.

Materials and methods

SWCNH characteristics

As previously reported (Li et al., 2010), SWCNH was synthesized using method of arc discharge method, and then dried at 100°C in air. The analysis of C, H, N analysis was conducted with the elemental analyzer (Vario EL III). X-ray fluorescence spectrometer (S4-Explorer) was used to measure the other elements. The mesopore size and surface area of SWCNH were also detected with the surface area analyzer (ASAP2010 V3.02E) based on the method of B.E.T. Moreover, the AccuPyc 1330 pycnometer was used to determine the density of SWCNH particle. Besides, SWCNH particle size was measured with Zetasizer Nano ZS at 298.3K based on the dynamic light scattering.

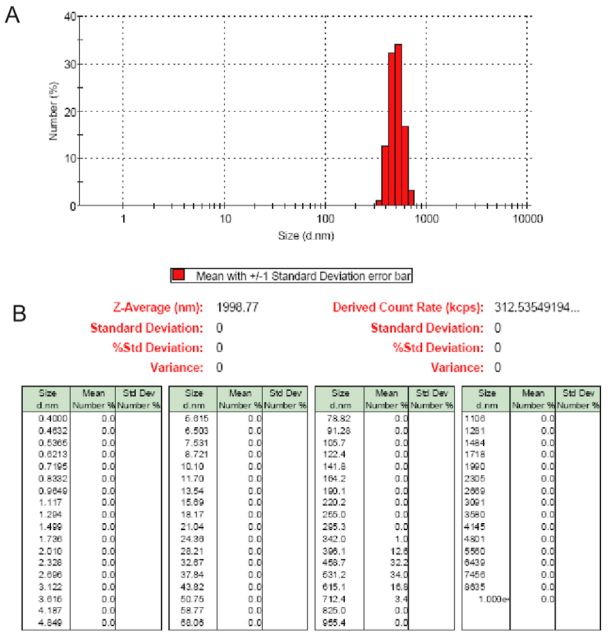

FIGURE 1
(A) Particle sizes (diameter.nm) distribution of SWCNH in aqueous suspension (10 μg/ml). **(B)** The particle number distribution showed that particle sizes of SWCNH in aqueous suspension ranged from 342 to 712 nm.

Characterization of dishes coated with SWCNH

The culture dishes were prepared with dispersed SWCNH, which was firstly soluted using ultrapure water. Normal PS (polystyrene dish) was 60-mm, and spotted with the dispersed SWCNH aliquot (10 μg/mL). Furthermore, these dishes were dried in air at 60°C, then sterilized utilizing UV irradiation.

Besides, PS dishes coated with SWCNH (0.85 $\mu g/cm^2$) were performed SEM measurements based on SIRION field emission scanning electronic microscope.

Cell culture

The poorly differentiated human NPC cell line CNE2 (CBP60003) was obtained from the Cell Bank of Type Culture Collection of Chinese Academy of Sciences (Shanghai, China). CNE2 was cultured with RPMI-1640 + 10% fetal bovine serum using the above dishes coated with SWCNH.

Cell synchronization and mitotic index

Mitotic events were scored by time-lapse video microscopy and DNA staining. The cells were synchronized as described above and

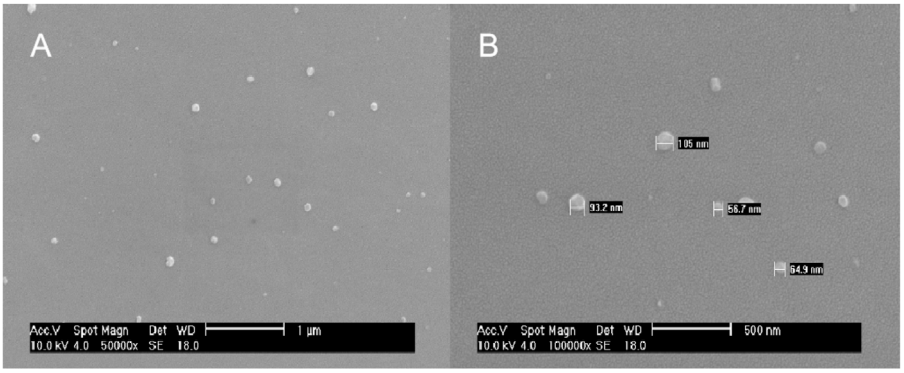

FIGURE 2
The films of SWCNH/PS observed by SEM. The SEM of films showed that SWCNH on PS surface (0.85 μg/cm^2) were individual spherical particles with diameters of 60–100 nm. **(A)** 500,00×, scale bar represents 1 μm. **(B)** 1,000,00×, scale bar represents 500 nm.

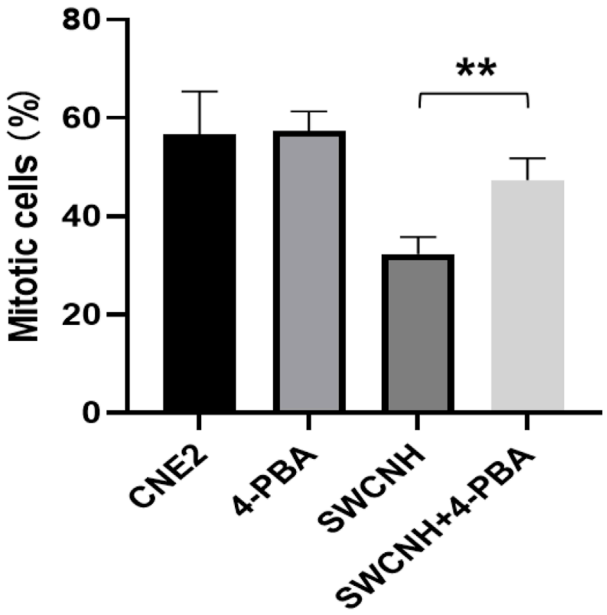

FIGURE 3
SWCNH inhibited mitotic entry of CNE2 cells. The rate of mitotic entry of CNE2 cells in SWCNH group and SWCNH +4-PBA group were lower compared to the control group. Moreover, the rate of mitotic entry of CNE2 cells in SWCNH group was also lower compared to SWCNH+4-PBA group ($p < 0.05$). But, the rate of mitotic entry of CNE2 cells in 4-PBA group was similar to the control group ($p > 0.05$). 4-phenylbutyrate (4-PBA) was selected as a inhibitor of ERS.

then cultured in SWNH-coated for 48 h. Real-time images were captured every 10 min with Openlab software (PerkinElmer Inc., Waltham, MA, USA). Mitotic events of control, cells were scored by their morphological change (from flat to round-up). For each experiment, at least 800 cells were videotaped, tracked, and analyzed. Alternatively, nocodazole (100 ng/mL) was added into the medium and after release, the cells were collected, fixed, and stained with DNA dye (Hoechst 33,258; Invitrogen, Carlsbad, CA, USA). Mitotic cells were scored by nuclear morphology and DNA condensation.

Cell apoptosis

After 48 h of co-culture, the adherent CNE2 cells were digested by trypsin and gently blown into a single cell suspension by suction tube. In each group, 1×10^6 cells were collected, and 0.1 mol/L phosphate buffer (PBS) was added. After centrifugal washing twice, the binding buffer, propidium iodide, 7-AAD and/or annexin V-fluorescein isothiocyanate were added respectively. Reaction under dark conditions for 25 min, then the apoptotic rate was determined with flow cytometry.

Caspase-3 expression

After 48 h of co-culture, the adherent CNE2 cells were digested by trypsin and gently blown into a single cell suspension by suction tube. In each group, 1×10^6 cells were collected. Reaction on ice for 40 min after adding cell lysate, then the protein supernatants were transferred into a novel tube and stored in the environment of −80°C after centrifugation for 10 min with 12, 000 r/min at 4°C. BCA protein concentration detection kit was used to detect the concentration of protein samples. The samples were fully denatured in water bath at 100°C for 5 min 40 μg denatured protein sample was added into each pore, the initial electrophoretic voltage was 80V. When bromophenol blue entered the junction of separating gel and concentrating gel, the voltage was adjusted to 120 V. When bromophenol blue entered the bottom edge of separating gel, the electrophoresis was completed. The protein was transferred for 90 min at 90 V. After sealing with skimmed milk, it was incubated overnight with 1:1,000 diluted caspase three antibody, and reacted with 1:2,000 diluted second antibody at room temperature for 60 min. The expression of caspase three was analyzed by taking β-actin as internal reference after exposing.

ROS level

After 48 h of co-culture, CNE2 cells were digested by trypsin and 1×10^6 cells were collected from each group. 2′, 7′-dichlorofluorescent yellow diacetate diluted with serum-free

10.3389/fmats.2024.1455648

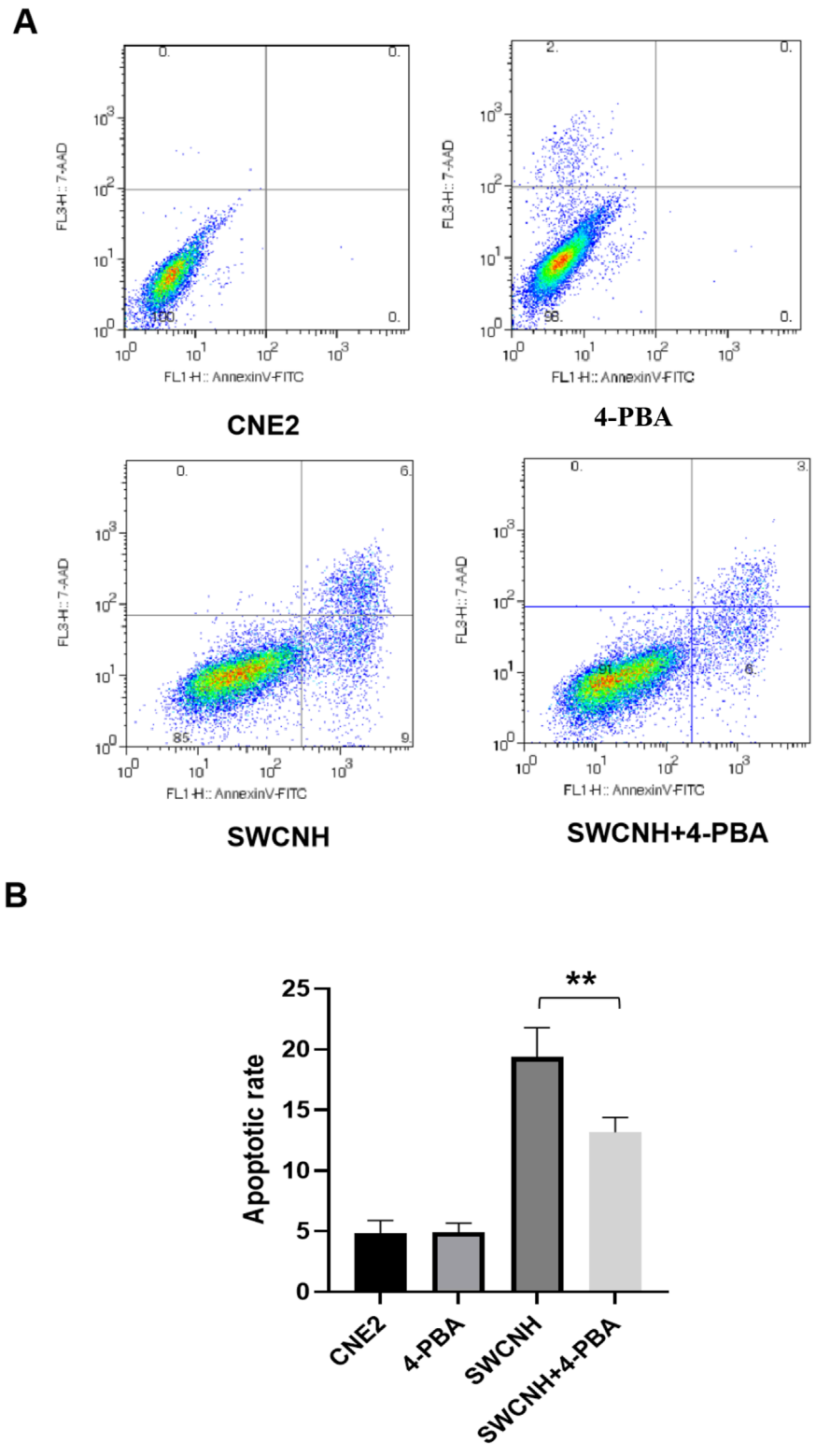

FIGURE 4
SWCNH induced apoptosis of CNE2 cells. The apoptotic rate of CNE2 cells in SWCNH group and SWCNH +4-PBA group was higher than that in control group. The apoptotic rate of CNE2 cells in SWCNH group was higher than that in SWCNH+4-PBA group ($p < 0.05$). The apoptotic rate of CNE2 cells in 4-PBA group was not significantly different from that in control group ($p > 0.05$). All experiments were conducted three times. **(A)** Distribution map of apoptotic cells detected by flow cytometry; **(B)** Percentage of apoptotic cells detected by flow cytometry.

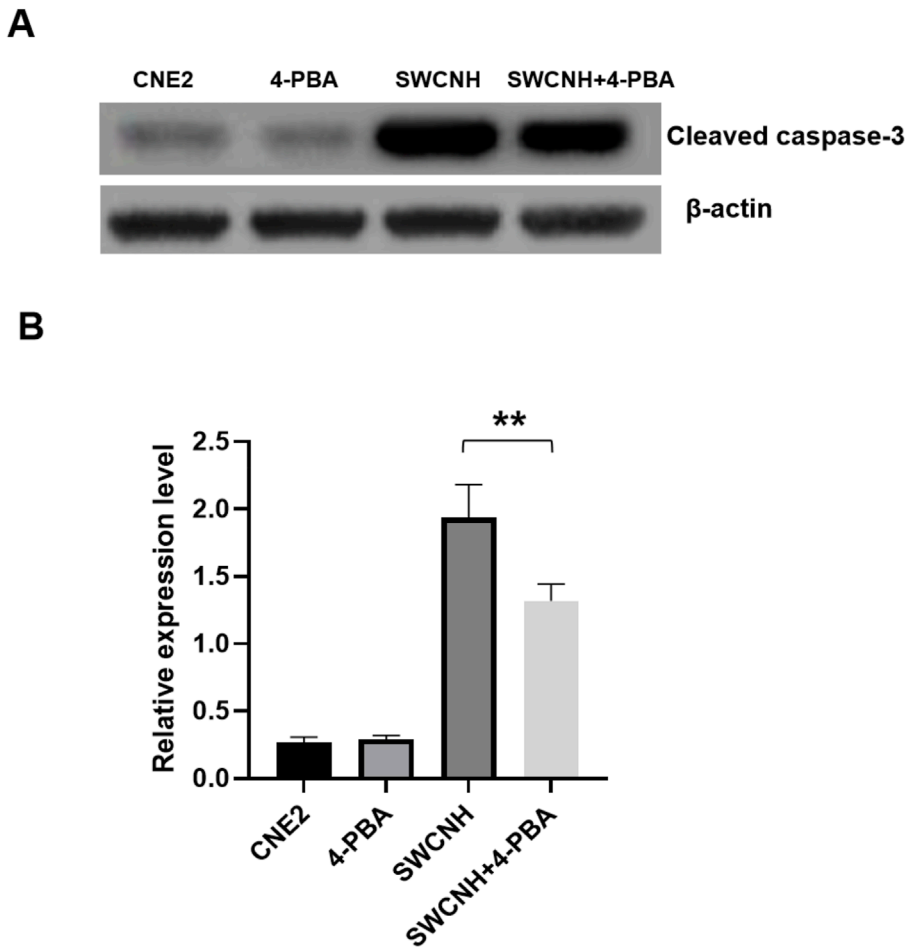

FIGURE 5
Over-expression of caspase-3 induced by SWCNH. The caspase three expression of apoptotic protein in SWCNH group and SWCNH+4-PBA group was higher than that in control group. The caspase three expression level in SWCNH group was higher than that in SWCNH+4-PBA group. The difference was statistically significant ($p < 0.05$). There was no significant difference in caspase three expression between 4-PBA group and control group ($p > 0.05$). All experiments were conducted three times. **(A)** The expression levels of cleaved caspase-3 detected by western blot; **(B)** The grayscale analysis of the expression levels of caspase-3 in A.

medium was added to each tube, and the final volume of each tube was 100 μL, incubated at 37°C for 20 min, washed twice with PBS, and then tested with flow cytometry.

The expression levels of ER pathway proteins

After 48 h of co-culture, proteins were extracted from CNE2 cells. ERS marker proteins eIF2α, ATF4, CHOP and OS-related proteins NQO-1, GCLC, HO-1, and Nrf2 expression levels were detected Western blot method. Moreover, 4-phenylbutyrate (4-PBA) was selected as a inhibitor of ERS.

Statistical methods

All data (mean ± standard deviation) were analyzed with SPSS statistical analysis software (version 20.0). $p < 0.05$ presented statistically significant.

Results

SWCNH characterization

At first, the distribution of particle size or density, the surface adsorptive isothem, and elemental composition were detected. Then, 95.3% C was found in this material, and each metals was less than 0.1% content, such as Cu (0.0396%), Cr (0.004%), and Fe (0.0863%), etc. Furthermore, 631.55 m^2/g was the surface area of SWCNH with B.E.T method according to the adsorptive isotherm plot (Supplementary Figure S1) (Murata et al., 2000). Besides, at P/Po 0.994, the diameter was less than 308.7 nm, at the same time, the total pore volume in single point was 1.57 cm^3/g. Moreover, the density of this particle was 1.0077 g/cm^3, RSD was 0.91%. It implied many closed pores existed in the material. The distribution of SWCNH was showed in Figure 1, which demonstrated the particle size was ranged from 342 to 712 nm in this aqueous suspension. The diameter of the individual SWCNH particle was 80–100 nm, and which was a dalia-like spherical nanohorns aggregate. Thus, in

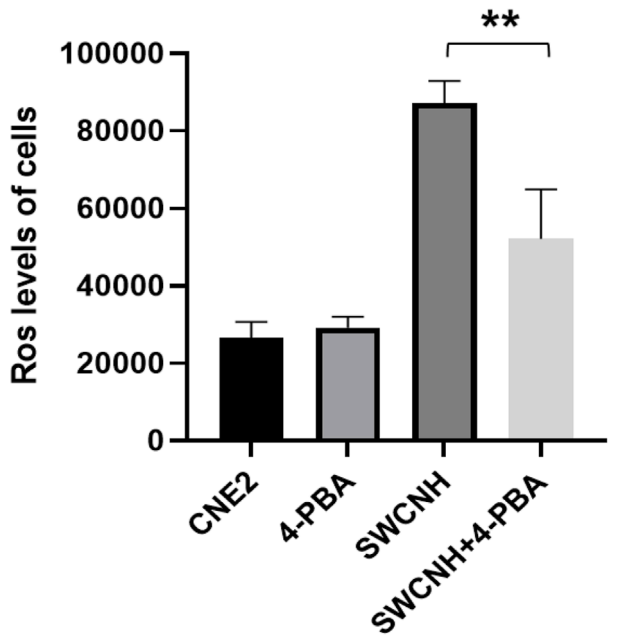

FIGURE 6
SWCNH affected the ROS levels of CNE2 cells. The ROS levels of CNE2 cells in SWCNH group and SWCNH+4-PBA group were higher than those in control group. The ROS levels of CNE2 cells in SWCNH group were higher than those in SWCNH+4-PBA group ($p < 0.05$). There was no significant difference in ROS levels between 4-PBA group and control group ($p > 0.05$). All experiments were conducted three times.

the aqueous suspension, SWCNH particles were the unit spherical aggregations. Secondly, the images of SEM confirmed that the diameters of this individual spherical SWCNH particles in PS surface were 60–100 nm (Figure 2). Therefore, our results indicated the stronger interactions of π-π stacking on surface of PS was existed between SWCNH and the benzene ring.

SWCNH inhibited mitotic entry of CNE2 cells

The rate of mitotic entry of CNE2 cells in SWCNH group and SWCNH +4-PBA group were lower compared to the control group. Moreover, the rate of mitotic entry of CNE2 cells in SWCNH group was also lower compared to SWCNH+4-PBA group ($p < 0.05$). But, the rate of mitotic entry of CNE2 cells in 4-PBA group was similar to the control group ($p > 0.05$) (Figure 3). 4-phenylbutyrate (4-PBA) was selected as a inhibitor of ERS.

SWCNH induced apoptosis of CNE2 cells

CNE2 apoptotic rate in SWCNH group and SWCNH +4-PBA group were higher compared to the control group. Moreover, CNE2 apoptotic rate in SWCNH group was also higher compared to SWCNH+4-PBA group ($p < 0.05$). But, CNE2 apoptotic rate in 4-PBA group was similar to the control group ($p > 0.05$) (Figure 4). 4-phenylbutyrate (4-PBA) was selected as a inhibitor of ERS.

Over-expression of caspase-3 induced by SWCNH

The caspase three expression of apoptotic protein in SWCNH group and SWCNH+4-PBA group was higher than that in control group. The caspase three expression level in SWCNH group was higher than that in SWCNH+4-PBA group. The difference was statistically significant ($p < 0.05$). There was no significant difference in caspase three expression between 4-PBA group and control group ($p > 0.05$) (Figure 5).

SWCNH affected the ROS levels of CNE2 cells

The ROS levels of CNE2 cells in SWCNH group and SWCNH+4-PBA group were higher compared to the control group. ROS levels in CNE2 cells of SWCNH group were higher than those in SWCNH+4-PBA group ($p < 0.05$). But, ROS levels in 4-PBA group was similar to the control group ($p > 0.05$) (Figure 6).

The effects of SWCNH on ER pathway proteins expression

ER marker proteins expression of ATF4 and CHOP in CNE2 cells of SWCNH group and SWCNH+4-PBA group was higher compared to the control group. The ATF4 and CHOP expression levels in SWCNH group were higher compared to the SWCNH+4-PBA group. Moreover, there was statistically significant difference ($p < 0.05$). But, the expression of ATF4 and CHOP proteins in control group and 4-PBA group could not be found. Besides, it was similar to the eIF2α expression in CNE2 cells among SWCNH, 4-PBA, and SWCNH+4-PBA group ($p > 0.05$) (Figure 7).

The expression levels of oxidative stress-related proteins caused by SWCNH

The NQO1, GCLC, HO-1, and Nrf2 expression levels in CNE2 cells of SWCNH group were higher compared to the control group. The NQO1, GCLC, HO-1, and Nrf2 expression levels in SWCNH group were higher compared to the SWCNH+4-PBA group, with statistical significance ($p < 0.05$). The expression levels of Nrf2, HO-1, GCLC and NQO1 in 4-PBA group were similar to the control group ($p > 0.05$) (Figure 8).

Discussion

ERS could be caused by the low doses of maternal CB-NP (carbon black nanoparticle) in PVMs (brain perivascular macrophages). Moreover, it could reactive astrocytes around blood vessels of mouse brain. Furthermore, misfolded proteins accumulated and accompanied by ERS, and associated with perivascular neurodegeneration and abnormalities (Onoda et al., 2020).

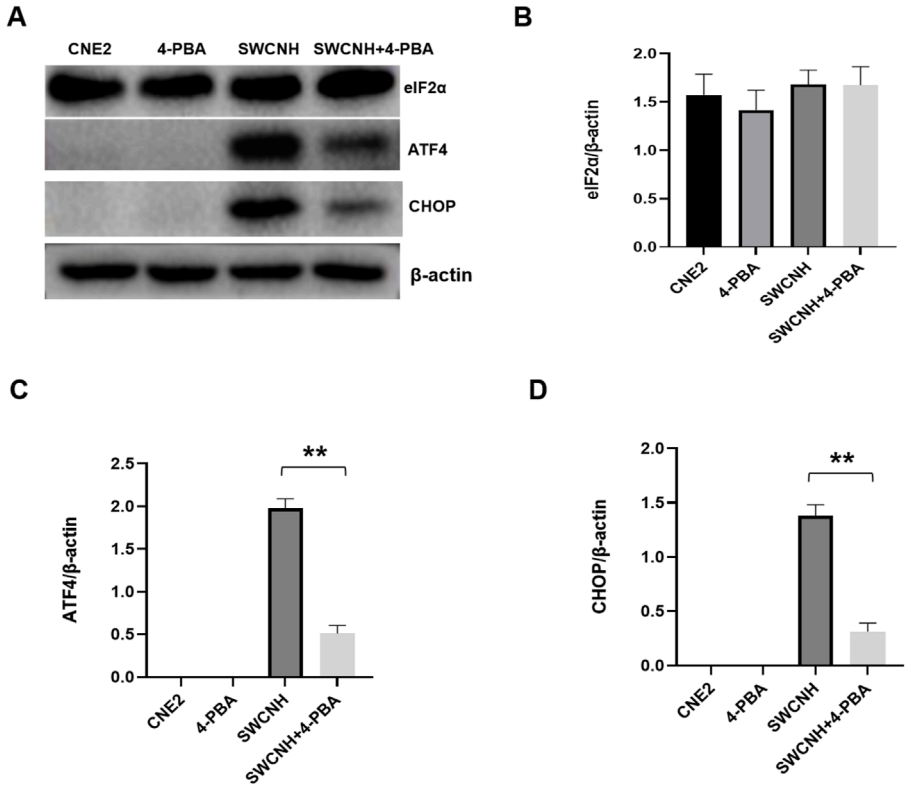

FIGURE 7
The effects of SWCNH on ER pathway proteins expression. The expression of ER marker proteins ATF4 and CHOP in CNE2 cells of SWCNH group and SWCNH+4-PBA group was higher than that of control group. The expression levels of ATF4 and CHOP in SWCNH group were higher than that in SWCNH+4-PBA group. The difference was statistically significant ($p < 0.05$). There was no expression of ATF4 and CHOP proteins in control group and 4-PBA group. There was no significant difference in eIF2α expression in CNE2 cells between SWCNH group, 4-PBA group and SWCNH+4-PBA group ($p > 0.05$). All experiments were conducted three times. **(A)** The expression levels of ER marker proteins detected by western blot; **(B)** The grayscale analysis of the expression levels of eIF2α in A; **(C)** The grayscale analysis of ATF4 expression levels in A; **(D)** The grayscale analysis of CHOP expression levels in A.

It was found that for rodents, SWCNH had low toxicity (Porter et al., 2007), and there was seldom report about its cytotoxicity (Miyawaki et al., 2008). Ajima et al. confirmed that SWNHox (oxidized SWCNH) could not inhibit proliferation of lung cancer cells (Ajima et al., 2005). Moreover, SWCNH modified with gum arabic did not suppress the viablility of Hela cells, too (Fan et al., 2007). In addition, oxSWCNH coated with DPEG could restrained growth of macrophage RAW 264.7 (Tahara et al., 2012). The above research results indicated different behaviors about cell functions, too. Which was associated with the type or characteristic of materials, including curvature, diameter, length, particle size, pore structure, and surface area, even cell types. Furthermore, the modified and unmodified nanomaterials of carbon based on different compounds and groups may induce different bio-effect on cells (Sohaebuddin et al., 2010).

As an important subcellular structure and functional unit of human body, endoplasmic reticulum is the common place for many kinds of intracellular and extracellular signal transduction (Oakes and Papa, 2015; Aitor et al., 2018). Under pathological conditions, endoplasmic reticulum produces a large number of unfolded or misfolded proteins and disorders of Ca^{2+} balance, which results in ERS. At the same time, cells initiate unfolded protein response (UPR) to restore the homeostasis of the cell's internal environment. When the time and intensity of ERS reach a certain level, UPR did not play a protective role (Seon et al., 2017; Rozpedek et al., 2016), and began to produce cytotoxic effects.

When ERS occurs, eIF2α is the initiation factor of translation will be phosphorylated, then promotes ATF4 (transcription factor), and activates CHOP (transcription factor) expression (Iurlaro and Cristina, 2016). Normally, CHOP mainly exists in the cytoplasm and is expressed at a low level. When cells are under stress, the expression of CHOP increases greatly and accumulates in the nucleus, which promotes the production of ROS. A large number of ROS also induces protein misfolding and Ca^{2+} imbalance in endoplasmic reticulum, which further stimulates the production of ROS and ERS (Cao and Kaufman, 2014). ROS includes superoxide anions, hydroxyl radicals and hydrogen peroxide, its production is related to ERS and UPR (Cao and Kaufman, 2014; Zheng et al., 2018). ROS plays a key role in many cell processes and can be produced in cytosol and various organelles including endoplasmic reticulum and mitochondria. The changes in the redox balance of endoplasmic reticulum are sufficient to induce ERS, which in turn induces the production of ROS in endoplasmic reticulum and mitochondria. Moreover, the persistent role of ROS causes oxidative stress damage, leading to NPC (Cai et al., 2021).

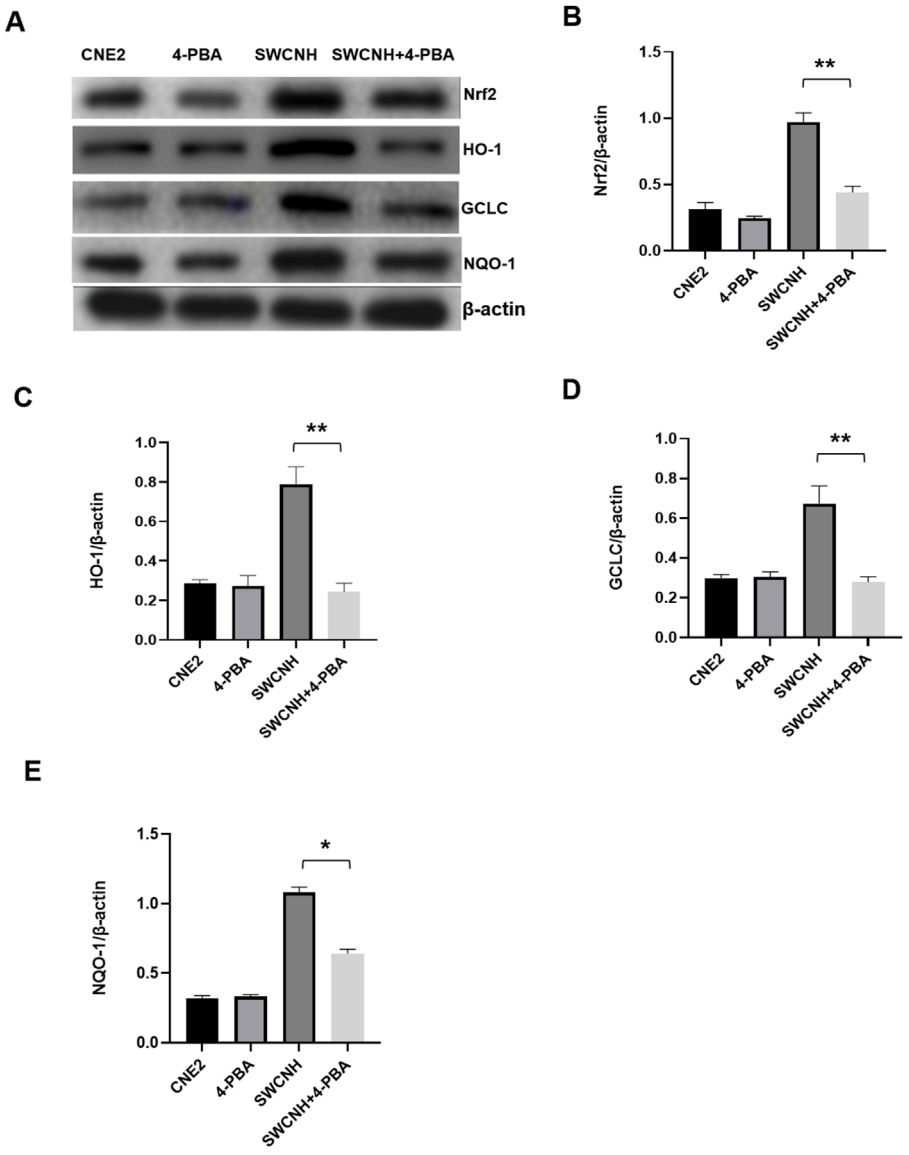

FIGURE 8
The expression levels of oxidative stress-related proteins caused by SWCNH. The expression levels of Nrf2, HO-1, GCLC and NQO1 in CNE2 cells of SWCNH group were higher than those of control group. The expression levels of Nrf2, HO-1, GCLC and NQO1 in SWCNH group were higher than those in SWCNH+4-PBA group, with statistical significance ($p < 0.05$). The expression levels of Nrf2, HO-1, GCLC and NQO1 in 4-PBA group were not significantly different from those in control group ($p > 0.05$). All experiments were conducted three times. **(A)** The expression levels of oxidative stress-related proteins detected by western blot; **(B)** The grayscale analysis of the expression levels of Nrf2 in A; **(C)** The grayscale analysis of HO-1 expression levels in A; **(D)** The grayscale analysis of GCLCexpression levels in A; **(E)** The grayscale analysis of NQO-1 expression in A.

Therefore, we explored the mechanism of ERS in apoptosis progression in CNE2 cell line. ERS in NPC cell line CNE2 was caused with SWCNH, and 4-phenylbutyrate (4-PBA) was selected as a inhibitor of ERS. CNE2 cells were co-cultured with SWCNH, 4-PBA and SWCNH+4-PBA, respectively. The expression levels of ER pathway protein eIF2α, ATF4 and CHOP, or OS-related proteins NQO1, GCLC, HO-1, and Nrf2 was detected. At first, our study confirmed that ER pathway proteins ATF4 and CHOP in SWCNH group and SWCNH+4-PBA group were higher compared to the control group. Moreover, these indicators were higher than that in SWCNH+4-PBA group, but these indicators in 4-PBA group was similar to the control group. ER (Endoplasmic reticulum) is the important cell organelle involved in the protein folding or modification in post-translational level, and assembly of membrane and secretory proteins in eukaryotic cells, and when these processes are affected, it can lead to Unfolded Protein Reaction (UPR) or misfolded proteins in ER. Reticulum accumulation causes ER stress (ERS), which is related to the pathophysiological processes of various human tumors, including tumor migration, invasion and metastasis (Cubillos-Ruiz et al., 2017). Solid tumors have three UPR pathways, PERK-eIF2α, IRE-1-XBP-1 and ATF6, and solid tumors activate UPR due to hypoxia. UPR makes tumor cells adapt to the stress state and survive by up-regulating the molecular chaperone GRP78/Bip in a more malignant direction. GRP78/Bip in NPC

enables tumor cells to survive through various mechanisms, and is closely related to tumor drug resistance and proliferation, invasion and metastasis (Liu et al., 2022). It is interesting that ERS induced by ROS maybe suppressed by deficiency of PERK, then which lead to apoptosis of tumor cells (Kim et al., 2008). Moreover, the activated c-Jun induced by ROS and ERS regulated cancer cells reciprocally (Su et al., 2012). Some findings indicated that ERS-mediated apoptosis might be one of potential mechanisms for cytotoxicity of cytotoxic substances (An et al., 2023; Xu et al., 2012; Liu et al., 2016).

SWCNH has the huge application prospects. Netheless, it is tremendous lack of studies on the mechanism and nanotoxicity of SWCNH. Moreover, SWCNH exhibits the clearly improved biocompatibility over carbon nanotubes (CNT) (Yuan et al., 2011). GPNMB (glycoprotein nonmetastatic melanoma protein B), the key transmembrane protein is discovered to initiate the nanotoxicity (He et al., 2018). At present, there is no literature reporting the biological effects of SWCNH on ROS and apoptosis. However, some researches has indicated the different role of SWCNTs (Single-walled carbon nanotubes). SWCNTs had apparent toxic effects to the protoplasts, including increased ROS generation, changed morphology, inducing apoptosis and necrosis of protoplast cells (Yuan et al., 2011). Furthermoe, Cheng et al. found the generation of ROS was dependent on activation of the mitochondria-apoptosis (Cheng et al., 2011). The apoptosis involved in a great deal of biochemical and morphological hallmarks, such as the activation of caspase-3, internucleosomal DNA fragmentation, chromatin condensation (Yang et al., 2014; Li et al., 2013). Besides, SWCNT could induce the breakage of DNA, the formation of micronuclei (MN), and suppress the growth of cell via the generation of ROS (Kim and Yu, 2014). Low doses of pristine and oxidized-SWCNTs affected mammalian embryonic development. SWCNT could cause genotoxicity, cytotoxicity, and ROS generation (Pietroiusti et al., 2011). SWNHs might be used as a safe anticancer agent, where it is able to trigger mitochondrial dysfunction-induced apoptosis by upregulating SIRT3 expression in HepG2 cells (Li et al., 2018). Although SWCNH are in early preclinical research yet, these nanotube-derived nanostructures demonstrate an interesting versatility pointing them out as promising forthcoming drug delivery systems to target and treat cancer cells (Moreno-Lanceta et al., 2020). The cytotoxicity and hemocompatibility studies prove that the studied materials are acceptable for use in biomedical applications, especially a sample SWCNH-ox-1.5 with the best application potential (Zieba et al., 2021).

In this study, the apoptotic status of CNE2 cells and its ROS levels of reactive oxygen species were determined, and the apoptotic protein expression of caspase 3, the expression levels of ER pathway protein eIF2α, ATF4 and CHOP, or OS-related proteins NQO1, GCLC, HO-1, and Nrf2 was detected. Finally, our study confirmed that CNE2 apoptotic rate, ROS levels, caspase three expression or ER pathway proteins ATF4 and CHOP, the OS-related proteins levels of NQO1, GCLC, HO-1, and Nrf2 in SWCNH group and SWCNH+4-PBA group were higher compared to the control group. Moreover, these indicators were higher than that in SWCNH+4-PBA group, but these indicators in 4-PBA group was similar to the control group.

Some of the known mechanisms describing the cytotoxicity of nanomaterials are as follows: 1) physical direct interaction of extremely sharp edges of nanomaterials with cell wall membrane (Akhavan and Ghaderi, 2010); 2) ROS generation (Taposhree et al., 2015) even in dark (Lakshmi Prasanna and Vijayaraghavan, 2015); 3) trapping the cells within the aggregated nanomaterials (Akhavan et al., 2011) for bacteria and (Ehsan et al., 2014) for spermatozoa; 4) oxidative stress (Liu et al., 2011); 5) interruption in the glycolysis process of the cells (Akhavan and Ghaderi, 2012); 6) DNA damaging (Ashutosh et al., 2011); 7) metal ion release (Wang et al., 2014); and recently 8) contribution in generation/explosion of nanobubbles (Jannesari et al., 2023). Therefore, the dominant mechanism occurred in this work should be ROS generation induced by SWCNH. Under pathological conditions, endoplasmic reticulum stress (ERS) occurs in endoplasmic reticulum, which produces a large number of unfolded or misfolded proteins and Ca^{2+} balance disorders. These kinds of processes can be controlled by designing effective anticancer proteins by using artificial intelligent-based methods.

Conclusion

ERS is the key apoptosis mechanism of CNE2 cells induced by SWCNH. After injury of ERS, SWCNH causes oxidative stress injury, which may eventually lead to apoptosis of CNE2 cells.

Data availability statement

The raw data supporting the conclusions of this article will be made available by the authors, without undue reservation.

Author contributions

XC: Conceptualization, Investigation, Software, Writing–original draft, Writing–review and editing. SG: Formal Analysis, Project administration, Validation, Writing–original draft, Writing–review and editing. SC: Data curation, Methodology, Supervision, Writing–original draft, Writing–review and editing. SH: Funding acquisition, Resources, Visualization, Writing–original draft, Writing–review and editing. TL: Conceptualization, Data curation, Formal Analysis, Writing–original draft, Writing–review and editing. YG: Methodology, Project administration, Validation, Writing–original draft, Writing–review and editing. CF: Software, Supervision, Validation, Visualization, Writing–original draft, Writing–review and editing. JZ: Conceptualization, Data curation, Formal Analysis, Funding acquisition, Writing–original draft, Writing–review and editing.

Funding

The author(s) declare that financial support was received for the research, authorship, and/or publication of this article. This work was supported by grants from the National Natural Science Foundation of China (No. 82360224), Yunnan Provincial Key Laboratory of Clinical Virology (202002AG070062, 202105AG070095, 202205AG070053), the Key Basic Research Program of Yunnan Province (No. 202201AS070065), and Kunming

University of Science and Technology Medical Joint Project (KUST-KH2022038Y). The study sponsors had no involvement in the work. The study sponsors had no involvement in the work.

Acknowledgments

The authors are grateful for the reviewer's valuable comments that improved the manuscript.

Conflict of interest

The authors declare that the research was conducted in the absence of any commercial or financial relationships that could be construed as a potential conflict of interest.

Publisher's note

All claims expressed in this article are solely those of the authors and do not necessarily represent those of their affiliated organizations, or those of the publisher, the editors and the reviewers. Any product that may be evaluated in this article, or claim that may be made by its manufacturer, is not guaranteed or endorsed by the publisher.

Supplementary material

The Supplementary Material for this article can be found online at: https://www.frontiersin.org/articles/10.3389/fmats.2024.1455648/full#supplementary-material

References

Aitor, A., Antonio, C., Chetan, C., Creedican, S., Doultsinos, D., Leuzzi, B., et al. (2018). Endoplasmic reticulum stress signalling – from basic mechanisms to clinical applications. *FEBS J.* 286, 241–278. doi:10.1111/febs.14608

Ajima, K., Murakami, T., Mizoguchi, Y., Tsuchida, K., Ichihashi, T., Iijima, S., et al. (2008). Enhancement of *in vivo* anticancer effects of cisplatin by incorporation inside single-wall carbon nanohorns. *ACS Nano* 2, 2057–2064. doi:10.1021/nn800395t

Ajima, K., Yudasaka, M., Murakami, T., Maigne, A., Shiba, K., and Iijima, S. (2005). Carbon nanohorns as anticancer drug carriers. *Mol. Pharm.* 2, 475–480. doi:10.1021/mp0500566

Akhavan, O., and Ghaderi, E. (2010). Toxicity of graphene and graphene oxide nanowalls against bacteria. *ACS Nano* 4, 5731–5736. doi:10.1021/nn101390x

Akhavan, O., and Ghaderi, E. (2012). *Escherichia coli* bacteria reduce graphene oxide to bactericidal graphene in a self-limiting manner. *Carbon* 50, 1853–1860. doi:10.1016/j.carbon.2011.12.035

Akhavan, O., Ghaderi, E., and Esfandiar, A. (2011). Wrapping bacteria by graphene nanosheets for isolation from environment, reactivation by sonication, and inactivation by near-infrared irradiation. *J. Phys. Chem. B* 115, 6279–6288. doi:10.1021/jp200686k

An, J., Du, C., Xue, W., Huang, J., Zhong, Y., Ren, G., et al. (2023). Endoplasmic reticulum stress participates in apoptosis of HeLa cells exposed to TPHP and OH-TPHP via the eIF2α-ATF4/ATF3-CHOP-DR5/P53 signaling pathway. *Toxicol. Res. (Camb)* 12, 1159–1170. doi:10.1093/toxres/tfad110

Ashutosh, K., Alok, K. P., Shashi, S. S., Rishi, S., and Alok, D. (2011). Engineered ZnO and TiO2 nanoparticles induce oxidative stress and DNA damage leading to reduced viability of *Escherichia coli*. *Free Radic. Biol. Med.* 51, 1872–1881. doi:10.1016/j.freeradbiomed.2011.08.025

Cai, J., Yi, M., Tan, Y., Li, X., Li, G., Zeng, Z., et al. (2021). Natural product triptolide induces GSDME-mediated pyroptosis in head and neck cancer through suppressing mitochondrial hexokinase-II. *J. Exp. Clin. Cancer Res.* 40, 190. doi:10.1186/s13046-021-01995-7

Cao, S. S., and Kaufman, R. J. (2014). Endoplasmic reticulum stress and oxidative stress in cell fate decision and human disease. *Antioxid. Redox Signal* 21, 396–413. doi:10.1089/ars.2014.5851

Chen, Y. P., Chan, A. T. C., Le, Q. T., Blanchard, P., Sun, Y., and Ma, J. (2019). Nasopharyngeal carcinoma. *Lancet* 394, 64–80. doi:10.1016/s0140-6736(19)30956-0

Cheng, W. W., Lin, Z. Q., Wei, B. F., Zeng, Q., Han, B., Wei, C. X., et al. (2011). Single-walled carbon nanotube induction of rat aortic endothelial cell apoptosis: reactive oxygen species are involved in the mitochondrial pathway. *Int. J. Biochem. Cell Biol.* 43, 564–572. doi:10.1016/j.biocel.2010.12.013

Cubillos-Ruiz, J. R., Bettigole, S. E., and Glimcher, L. H. (2017). Tumorigenic and immunosuppressive effects of endoplasmic reticulum stress in cancer. *Cell* 168, 692–706. doi:10.1016/j.cell.2016.12.004

Ehsan, H., Omid, A., Mehdi, S., Reza, R., Ali, E., and Aidin Rahim, T. (2014). Cyto and genotoxicities of graphene oxide and reduced graphene oxide sheets on spermatozoa. *RSC Adv.* 4, 27213–27223. doi:10.1039/c4ra01047g

Fan, X. B., Tan, J., Zhang, G. L., and Zhang, F. B. (2007). Isolation of carbon nanohorn assemblies and their potential for intracellular delivery. *Nanotechnology* 18, 195103–195108. doi:10.1088/0957-4484/18/19/195103

He, B., Shi, Y., Liang, Y., Yang, A., Fan, Z., Yuan, L., et al. (2018). Single-walled carbon-nanohorns improve biocompatibility over nanotubes by triggering less protein-initiated pyroptosis and apoptosis in macrophages. *Nat. Commun.* 9, 2393. doi:10.1038/s41467-018-04700-z

Iijima, S., Yudasaka, M., Yamada, R., Bandow, S., Suenaga, K., Kokai, F., et al. (1999). Nano-aggregates of single-walled graphitic carbon nano-horns. *Chem. Phys. Lett.* 309, 165–170. doi:10.1016/s0009-2614(99)00642-9

Iurlaro, R., and Cristina, M. P. (2016). Cell death induced by endoplasmic reticulum stress. *FEBS J.* 283, 2640–2652. doi:10.1111/febs.13598

Jannesari, M., Akhavan, O., Madaah Hosseini, H. R., and Bakhshi, B. (2023). Oxygen-Rich Graphene/ZnO2-Ag nanoframeworks with pH-Switchable Catalase/Peroxidase activity as O2 Nanobubble-Self generator for bacterial inactivation. *J. Colloid Interface Sci.* 637, 237–250. doi:10.1016/j.jcis.2023.01.079

Kim, I., Xu, W., and Reed, J. C. (2008). Cell death and endoplasmic reticulum stress: disease relevance and therapeutic opportunities. *Nat. Rev. Drug Discov.* 7, 1013–1030. doi:10.1038/nrd2755

Kim, J. S., and Yu, I. J. (2014). Single-wall carbon nanotubes (SWCNT) induce cytotoxicity and genotoxicity produced by reactive oxygen species (ROS) generation in phytohemagglutinin (PHA)-stimulated male human peripheral blood lymphocytes. *J. Toxicol. Environ. Health A* 77, 1141–1153. doi:10.1080/15287394.2014.917062

Lakshmi Prasanna, V., and Vijayaraghavan, R. (2015). Insight into the mechanism of antibacterial activity of ZnO: surface defects mediated reactive oxygen species even in the dark. *Langmuir* 31, 9155–9162. doi:10.1021/acs.langmuir.5b02266

Lenna, S., Han, R., and Trojanowska, M. (2014). Endoplasmic reticulum stress and endothelial dysfunction. *Iubmb Life* 66, 530–537. doi:10.1002/iub.1292

Li, B., Chen, X., Yang, W., He, J., He, K., Xia, Z., et al. (2018). Single-walled carbon nanohorn aggregates promotes mitochondrial dysfunction-induced apoptosis in hepatoblastoma cells by targeting SIRT3. *Int. J. Oncol.* 53, 1129–1137. doi:10.3892/ijo.2018.4459

Li, N., Wang, Z. Y., Zhao, K. K., Shi, Z. J., Gu, Z. N., and Xu, S. K. (2010). Synthesis of single-wall carbon nanohorns by arc-discharge in air and their formation mechanism. *Carbon* 48, 1580–1585. doi:10.1016/j.carbon.2009.12.055

Li, Y. J., Zhang, J. Q., Zhao, M., Shi, Z. J., Chen, X., He, X. H., et al. (2013). Single-wall carbon nanohorns (SWNHs) inhibited proliferation of human glioma cells and promoted its apoptosis. *J. Nanopart Res.* 15, 1861. doi:10.1007/s11051-013-1861-5

Liu, S., Li, Y., and Li, Z. (2022). Salidroside suppresses the activation of nasopharyngeal carcinoma cells via targeting miR-4262/GRP78 axis. *Cell Cycle* 21, 720–729. doi:10.1080/15384101.2021.2019976

Liu, S., Zeng, T. H., Hofmann, M., Burcombe, E., Wei, J., Jiang, R., et al. (2011). Antibacterial activity of graphite, graphite oxide, graphene oxide, and reduced graphene oxide: membrane and oxidative stress. *ACS Nano* 5, 6971–6980. doi:10.1021/nn202451x

Liu, Z., Shi, Q., Song, X., Wang, Y., Wang, Y., Song, E., et al. (2016). Activating transcription factor 4 (ATF4)-ATF3-C/EBP homologous protein (CHOP) cascade shows an essential role in the ER stress-induced sensitization of tetrachlorobenzoquinone-challenged PC12 cells to ROS-mediated apoptosis via death receptor 5 (DR5) signaling. *Chem. Res. Toxicol.* 29, 1510–1518. doi:10.1021/acs.chemrestox.6b00181

Malhotra, J. D., and Kaufman, R. J. (2007). The endoplasmic reticulum and the unfolded protein response. *Seminars Cell Dev. Biol.* 18, 716–731. doi:10.1016/j.semcdb.2007.09.003

Matsumura, S., Ajima, K., Yudasaka, M., Iijima, S., and Shiba, K. (2007). Dispersion of cisplatin-loaded carbon nanohorns with a conjugate comprised of an artificial peptide aptamer and polyethylene glycol. *Mol. Pharm.* 4, 723–729. doi:10.1021/mp070022t

Miyawaki, J., Yudasaka, M., Azami, T., Kubo, Y., and Iijima, S. (2008). Toxicity of single-walled carbon nanohorns. *ACS Nano* 2, 213–226. doi:10.1021/nn700185t

Moreno-Lanceta, A., Medrano-Bosch, M., and Melgar-Lesmes, P. (2020). Single-walled carbon nanohorns as promising nanotube-derived delivery systems to treat cancer. *Pharmaceutics* 12, 850. doi:10.3390/pharmaceutics12090850

Muracami, T., Savada, H., Tamura, G., Yudasaka, M., Iijima, S., and Tsuchida, K. (2008). Water-dispersed single-wall carbon nanohorns as drug carriers for local cancer chemotherapy. *Nanomedicine* 3, 453–463. doi:10.2217/17435889.3.4.453

Murakami, T., and Tsuchida, K. (2008). Recent advances in inorganic nanoparticle-based drug delivery systems. *Mini-Reviews Med. Chem.* 8, 175–183. doi:10.2174/138955708783498078

Murata, K., Kaneko, K., Kokai, F., Takahashi, K., Yudasaka, M., and Iijima, S. (2000). Pore structure of single-wall carbon nanohorn aggregates. *Chem. Phys. Lett.* 331, 14–20. doi:10.1016/s0009-2614(00)01152-0

Niedobitek, G. (2000). Epstein-Barr virus infection in the pathogenesis of nasopharyngeal carcinoma. *Mol. Pathol.* 53, 248–254. doi:10.1136/mp.53.5.248

Oakes, S. A., and Papa, F. R. (2015). The role of endoplasmic reticulum stress in human pathology. *Annu. Rev. Pathology* 10, 173–194. doi:10.1146/annurev-pathol-012513-104649

Onoda, A., Kawasaki, T., Tsukiyama, K., Takeda, K., and Umezawa, M. (2020). Carbon nanoparticles induce endoplasmic reticulum stress around blood vessels with accumulation of misfolded proteins in the developing brain of offspring. *Sci. Rep.* 10, 10028. doi:10.1038/s41598-020-66744-w

Pietroiusti, A., Massimiani, M., Fenoglio, I., Colonna, M., Valentini, F., Palleschi, G., et al. (2011). Low doses of pristine and oxidized single-wall carbon nanotubes affect mammalian embryonic development. *ACS Nano* 5, 4624–4633. doi:10.1021/nn200372g

Porter, A. E., Gass, M., Muller, K., Skepper, J. N., Midgley, P., and Welland, M. (2007). Visualizing the uptake of C60 to the cytoplasm and nucleus of human monocyte derived macrophage cells using energy-filtered transmission electron microscopy and electron tomography. *Environ. Sci. Technol.* 41, 3012–3017. doi:10.1021/es062541f

Rozpedek, W., Pytel, D., Mucha, B., Leszczynska, H., Diehl, J., and Majsterek, I. (2016). The role of the PERK/eIF2α/ATF4/CHOP signaling pathway in tumor progression during endoplasmic reticulum stress. *Curr. Mol. Med.* 16, 533–544. doi:10.2174/1566524016666160523143937

Seon, Y. Y., Gyeong, H. H., and Joo, J. Y. (2017). Unfolded protein response of the endoplasmic reticulum in tumor progression and immunogenicity. *Oxidative Med. Cell. Longev.* 2017, 2969271. doi:10.1155/2017/2969271

Siegel, R. L., Miller, K. D., Fuchs, H. E., and Jemal, A. (2021). Cancer statistics, 2021. *CA Cancer J. Clin.* 71, 7–33. doi:10.3322/caac.21654

Sohaebuddin, S. K., Thevenot, P. T., Baker, D., Eaton, J. W., and Tang, L. P. (2010). Nanomaterial cytotoxicity is composition, size, and cell type dependent. *Part. Fibre Toxicol.* 7, 22. doi:10.1186/1743-8977-7-22

Su, T. R., Tsai, F. J., Lin, J. J., Huang, H. H., Chiu, C. C., Su, J. H., et al. (2012). Induction of apoptosis by 11-dehydrosinulariolide via mitochondrial dysregulation and ER stress pathways in human melanoma cells. *Mar. Drugs* 10, 1883–1898. doi:10.3390/md10081883

Tahara, Y., Nakamura, M., Yang, M., Zhang, M., Iijima, S., and Yudasaka, M. (2012). Lysosomal membrane destabilization induced by high accumulation of single-walled carbon nanohorns in murine macrophage RAW 264.7. *Biomaterials* 33, 2762–2769. doi:10.1016/j.biomaterials.2011.12.023

Taposhree, D., Rudra, S., Bholanath, P., Subrata, G., Ripon, S., Ananya, B., et al. (2015). ROS generation by reduced graphene oxide (rGO) induced by visible light showing antibacterial activity: comparison with graphene oxide (GO). *RSC Adv.* 5, 80192–80195. doi:10.1039/c5ra14061g

Wang, Y. W., Cao, A., Jiang, Y., Zhang, X., Liu, J. H., Liu, Y., et al. (2014). Superior antibacterial activity of zinc oxide/graphene oxide composites originating from high zinc concentration localized around bacteria. *ACS Appl. Mater Interfaces* 6, 2791–2798. doi:10.1021/am4053317

Xu, J. X., Yudasaka, M., Kouraba, S., Sekido, M., Yamamoto, Y., and Iijima, S. (2008). Single wall carbon nanohorn as a drug carrier for controlled release. *Chem. Phys. Lett.* 461, 189–192. doi:10.1016/j.cplett.2008.06.077

Xu, L., Su, L., and Liu, X. (2012). PKCδ regulates death receptor 5 expression induced by PS-341 through ATF4-ATF3/CHOP axis in human lung cancer cells. *Mol. Cancer Ther.* 11, 2174–2182. doi:10.1158/1535-7163.mct-12-0602

Yang, M., Zhang, M., Tahara, Y., Chechetka, S., Miyako, E., Iijima, S., et al. (2014). Lysosomal membrane permeabilization: carbon nanohorn-induced reactive oxygen species generation and toxicity by this neglected mechanism. *Toxicol. Appl. Pharm.* 280, 117–126. doi:10.1016/j.taap.2014.07.022

Yuan, H., Hu, S., Huang, P., Song, H., Wang, K., Ruan, J., et al. (2011). Single walled carbon nanotubes exhibit dual-phase regulation to exposed arabidopsis mesophyll cells. *Nanoscale Res. Lett.* 6, 44. doi:10.1007/s11671-010-9799-3

Zheng, W., Wang, B., Si, M., Zou, H., Song, R., Gu, J., et al. (2018). Zearalenone altered the cytoskeletal structure via ER stress-autophagy- oxidative stress pathway in mouse TM4 Sertoli cells. *Sci. Rep.* 8, 3320. doi:10.1038/s41598-018-21567-8

Zheng, Z. Q., Li, Z. X., Zhou, G. Q., Lin, L., Zhang, L. L., Lv, J. W., et al. (2019). Long noncoding RNA FAM225A promotes nasopharyngeal carcinoma tumorigenesis and metastasis by acting as ceRNA to sponge miR-590-3p/miR-1275 and upregulate ITGB3. *Cancer Res.* 79, 4612–4626. doi:10.1158/0008-5472.can-19-0799

Zieba, W., Czarnecka, J., Rusak, T., Zieba, M., and Terzyk, A. P. (2021). Nitric-acid oxidized single-walled carbon nanohorns as a potential material for bio-applications-toxicity and hemocompatibility studies. *Mater. (Basel)* 14, 1419. doi:10.3390/ma14061419